JOURNAL OF MATERIALS SCIENCE 5 (1970) 133-140

Corrugated Bicrystal Grain-Boundaries in Cast Aluminium and Zinc

T. R. ANTHONY, J. L. WALTER
General Electric Research and Development Centre, Schenectady, New York, USA

A ridging or corrugation structure has been found to form on grain-boundary surfaces in zinc and aluminium parallel to the solidification direction. The density and severity of this ridging is found to increase with increasing solidification rates. The ridging is associated with substructure in the bicrystals forming the grain-boundary. Previous experiments suggest that this ridging can impart a considerable amount of resistance to grain-boundary sliding perpendicular to the solidification direction.

1. Introduction

Many of the experiments designed to measure rates of grain-boundary sliding have utilised boundaries in bicrystals [1-3] and tricrystals [4, 5] grown from the melt. The configuration of the grain-boundary (flat, curved, rumpled, etc.) may be expected to influence grain-boundary sliding rates [6-8]. The possibility exists that some of the ambiguity found in measured sliding rates may be the result of sliding on non-flat or non-spherically curved boundaries. The exact grain-boundary configuration should determine whether grain-boundary shear is accomplished by "pure sliding", shearing or creep in the grains contiguous with the boundary and/or grain-boundary migration [7-10].

Puttick and King [1] have shown that there is a significant difference between the grain-boundary configuration in as-cast and recrystallised tin of the same purity; the as-cast grain-boundaries had fine corrugations while the boundaries of recrystallised tin were smooth. They also observed that the grain-boundary corrugations appearing in the as-cast material disappeared with increasing purity of their tin.

Recent experiments in this laboratory indicated that grain-boundary corrugations appeared even in very high purity aluminium and zinc if the solidification rate was sufficiently high. Consequently, we have prepared bicrystals of zinc and aluminium, grown at various rates from the melt, to determine the effect of solidification rates on the configuration of the bicrystal boundaries. The results indicate that grain-boundary corrugations may be a phenomenon associated with most materials grown from the melt. The presence of corrugations suggests an explanation of the observation that metals in the as-cast condition often have greater creep resistance than wrought-and-annealed materials.

2. Experimental

2.1. Zinc

Single crystals of zinc (99.999% purity) were grown in horizontal graphite boats by the moving furnace method [11]. Two such single crystals were used to grow bicrystals of zinc in horizontal graphite boats described elsewhere [12]. The bicrystals were grown at rates of 2 cm h^{-1} and 20 cm h^{-1}. The position of the bicrystal boundary is shown with respect to the bicrystal shape in fig. 1.

Following completion of crystal growth, the bicrystal was separated along its boundary by coating a thin layer of liquid gallium on the intersection of the boundary and the free surface and applying a small bending moment across the boundary. The wetting of the zinc by the gallium was facilitated by first treating the area of interest with acetic acid.

Because of the intergranular embrittling properties of the gallium, the zinc bicrystal parted immediately along its boundary. Excess gallium was removed by repeated blotting with Scotch tape. The exposed grain-boundary was then examined for structure.

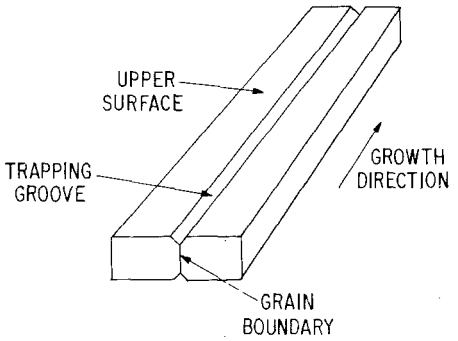

Figure 1 Drawing of bicrystal shape and position of the grain-boundary of the bicrystal.

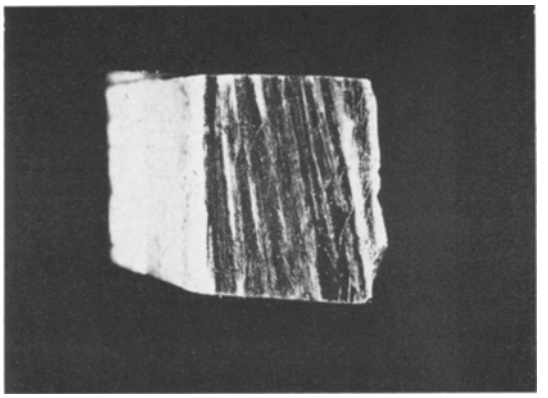

Figure 2 Ridging on a zinc grain-boundary separated by liquid gallium (×3).

2.2. Aluminium

Two single crystals of aluminium were used to grow bicrystals of aluminium (99.9998% purity) with a twenty degree tilt around a ⟨100⟩ direction by the method described previously for zinc. The bicrystal was grown so that the tilt axis was perpendicular to the growth direction. The growth rate used to grow the bicrystals was varied from 2 cm h^{-1} to 160 cm h^{-1}. In several bicrystals, two different growth rates were used for different sections of the same bicrystal.

The grain-boundary structure of the aluminium bicrystals was examined by several methods. First, a series of cross-sectional cuts of the bicrystal were taken perpendicular to the solidification direction. From these slices, the profile of the boundary was determined by light microscopy. Laue X-ray patterns and Berg-Barrett photographs were made of the adjoining grains to measure the angular misorientation of subgrains and to determine whether there was any association between the grain-boundary structure and the possible substructure of these grains. Several sections which showed pronounced boundary structure were annealed at 630° C for several days to determine the effects of prolonged annealing on boundary structure. In addition, several sections were strained and annealed so that the grain-boundaries of recrystallised grains in the same material could be examined.

Finally, entire aluminium bicrystals were separated along their boundaries by using the technique of liquid gallium grain-boundary embrittlement. After removal of excess gallium, the resulting exposed boundaries were examined for any boundary structure present.

3. Results

3.1. Zinc

Fig. 2 shows an example of type of boundary structure found in zinc bicrystals grown from the melt at high growth rates. At high growth rates (20 cm h^{-1}) a very pronounced corrugation structure was produced parallel to the growth direction. At low growth rates (3 cm h^{-1}), the boundary was relatively flat and smooth. Nevertheless, a definite pattern of widely separated small ridges developed parallel to the solidification direction.

The ridges in both the low- and high-speed growth conditions were associated with substructure in the grains forming the bicrystal boundary. However, under high-speed growth conditions, the dihedral angle formed by these ridges did not satisfy an equilibrium balance of surface tensions between the substructure and main boundary. Instead, the ridges were much sharper and deeper.

3.2. Aluminium

Fig. 3 shows the typical grain-boundary configuration in aluminium bicrystals grown from the melt at different rates. The extreme left end of fig. 3a shows the part of the boundary first grown at 3 cm h^{-1}. The right-hand side of figs. 3a and b show the boundary in that length of the bicrystal where the growth rate was increased to 160 cm h^{-1}. The section shown in fig. 3c is that part of the boundary formed when the growth rate was reduced from 160 to 3 cm h^{-1}.

In the first slow growth area (fig. 3a), the boundary is fairly smooth in appearance. At higher magnification, however (fig. 4), the

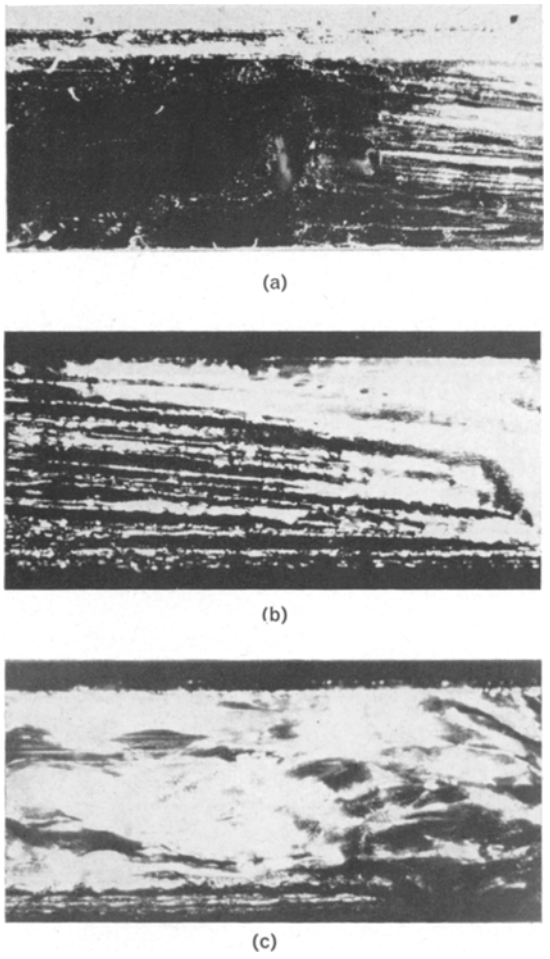

Figure 3 Consecutive sections of an aluminium bicrystal boundary separated by liquid gallium. (a) Growth rate 3 cm h^{-1}. (b) Growth rate increased to 160 cm h^{-1}. (c) Growth rate reduced back to 3 cm h^{-1} (×4).

boundary is seen to be formed of smooth facets with sharp ridges where the tilted facets meet. In the fast growth zone (fig. 3b), the boundary becomes corrugated with the ridges running parallel to the direction of growth. The corrugated boundary is shown in an exaggerated schematic illustration in fig. 5 (the photograph does not effectively delineate the actual degree of ridging). These corrugations were both deeper and sharper than would be expected if surface tensions had been balanced between the main boundary and intersecting sub-boundaries.

In the second slow growth zone the boundary does not return to the configuration obtained

*1 in. = 2.54 cm.

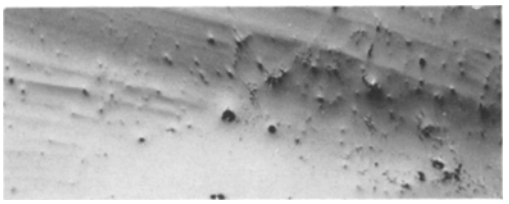

Figure 4 Grain-boundary faceting in aluminium in the initial slow growth zone of fig. 3a (× 93).

for the first slow growth region. Instead, the corrugations diminish to a jumble of facets as may be seen in fig. 3c.

One of the bicrystals was cross-sectioned at $\frac{1}{2}$ in.* intervals along its length. A cross-section of the bicrystal boundary in the fast growth section is shown in fig. 6. A series of X-ray back-reflection Laue diffraction patterns was taken along the boundary in one of the grains. The misorientations along the boundary in the fast growth region amounted to less than $\frac{1}{2}°$.

Optical microscopy only occasionally revealed substructure in samples first anodised, then viewed in polarised light. An example of subgrains intersecting a grain-boundary at various points is given in fig. 7. It is apparent that substructure existed in only one grain; the grain containing the centre of curvature of the boundary was free of substructure. Because of the frequent failure of conventional anodising and etching techniques to reveal any substructure, the subgrains were decorated with vacancy pits by annealing these cross-sections in air at 630° C and cooling to room temperature [13]. The sub-boundaries and main boundaries which act as efficient vacancy sinks stood out distinctly as pit-free regions forming an irregular pencil-like structure parallel to the direction of growth. The subgrains decreased in size with increasing

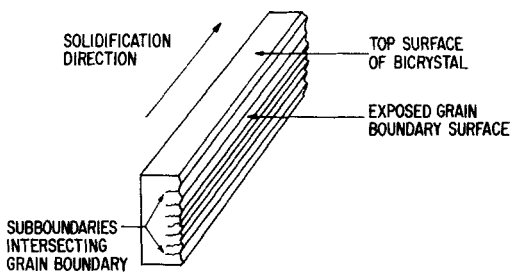

Figure 5 Drawing of grain-boundary ridging induced by high solidification rates.

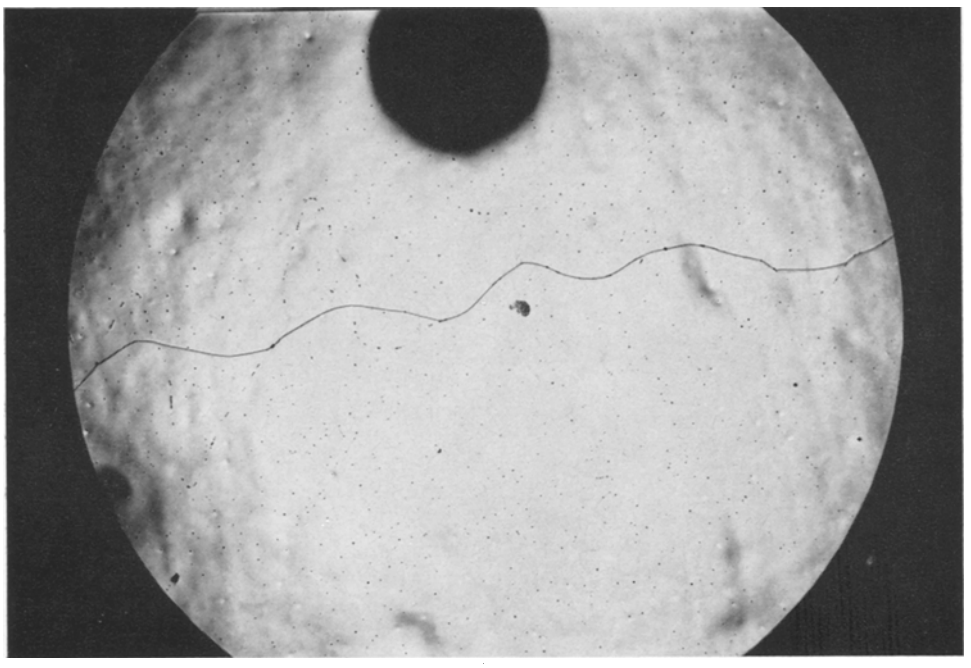

Figure 6 Cross-section of an aluminium bicrystal boundary in fast growth zone of fig. 3b (×36).

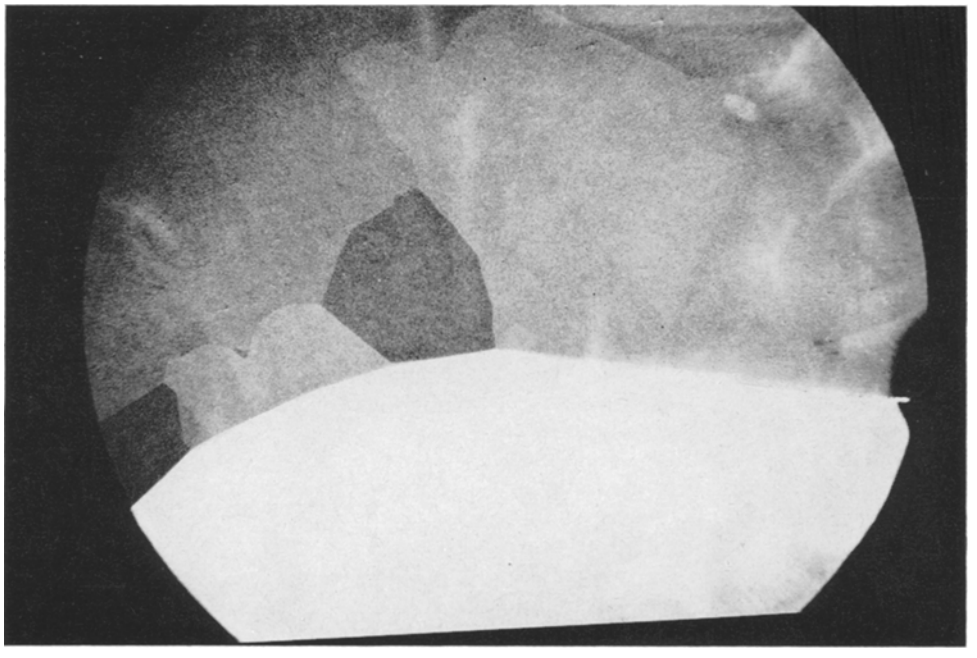

Figure 7 Subgrains causing faceting of an aluminium bicrystal boundary (×36).

growth rates. It was also seen that the cusps of the corrugated boundary structure running parallel to the growth direction were associated with the intersection of sub-boundaries with the main boundary (fig. 8).

Prolonged annealing near the melting point of the aluminium had no effect on the corrugated structure of the grain-boundary. Recrystallisation, on the other hand, generated new grain-boundaries with a markedly different configura-

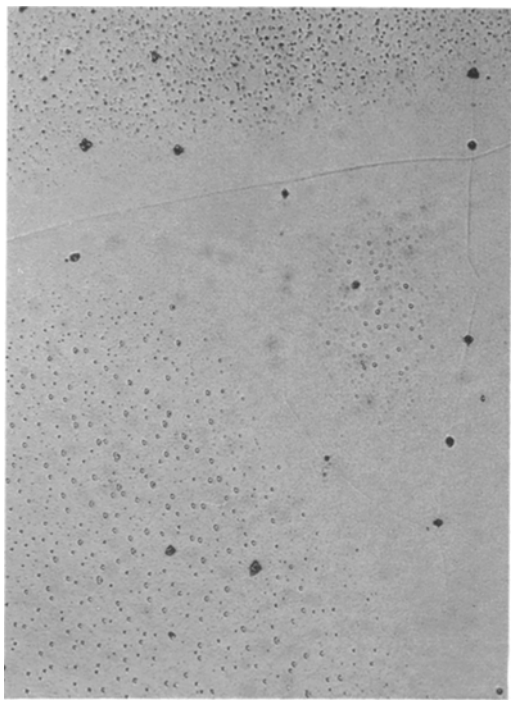

Figure 8 Association of crystal substructure in aluminium with cusps on grain-boundaries revealed by vacancy-condensation-pit etching. (×250)

tion. Several bicrystals with deeply corrugated boundaries were strained by bending. When annealed, these specimens recrystallised. The boundaries of the recrystallised grains, after separation with gallium, were smooth and ridge free. This finding demonstrates that boundary corrugations are formed in the solidification process and are not an inherent characteristic of the material.

4. Discussion

4.1. Zinc

The occurrence of substructure running parallel to the direction of solidification in zinc crystals is well documented in the literature [14-19]. It has been found that the size of the subgrains decreases with increasing solidification rate while the angular misorientation between subgrains or lineage boundaries remains constant [15]. Under slow growth conditions, the boundary ridging parallel to the solidification direction is simply the result of the intersection of sub-structure with the main boundary. The actual profile of the ridging will conform to a balance of surface tensions between the sub-boundaries and the main boundary.

Because the angular misorientation between subgrains is independent of the solidification rate, one would expect under conditions of fast growth that while the density of ridging would increase to match the decrease in subgrain size, the dihedral angle of the ridging would remain unchanged. The contrary observation of a more pronounced ridging implies that some sort of metastable equilibrium must exist.

Fig. 9a shows a schematic diagram of sub-boundaries and the main boundary in a cross-sectional view of a bicrystal perpendicular to the growth direction. If the sub-boundaries and main boundaries had equal mobilities, then sub-boundaries I and II would gradually migrate toward each other while sub-boundary III would lengthen. The end result would be as shown in fig. 9b. However, it is known that striations and substructure are very stable in a crystal and will remain unchanged if a crystal is held near its melting point for several days. If the substructure formed a perfect hexagonal array, one could simply ascribe its stability to a perfect balance of surface tensions. However, in many cases, the substructure has a very irregular shape [20]. Thus, the stability of the substructure must be a result of the low mobility of these low-angle boundaries [21].

If we assume that the high-angle bicrystal boundary has a much greater mobility than the substructure boundaries, then the increase in the sharpness of boundary ridging with higher growth rates can be explained. At high growth rates, the substructure spacing becomes smaller and conditions diagrammed in fig. 9a are encountered. If

$$\frac{\gamma_{sub}}{\gamma_m} > \frac{2y - x}{2y},$$

then the energy of the configuration shown in fig. 9a can be lowered if the main boundary migrates towards the nodal point A of the substructure and finally assumes the position shown in fig. 9c. Here γ_{sub} and γ_m are the energies of the sub-boundary and main boundary respectively and x and y are the respective lengths of the main boundary and sub-boundary sections shown in fig. 9a. Following migration of the mobile main boundary, the grain-boundary surface ridging will reflect the morphology of the substructure rather than a surface tension equilibrium between the main boundary and the widely spaced substructure found under slow growth conditions. In this manner, the increased

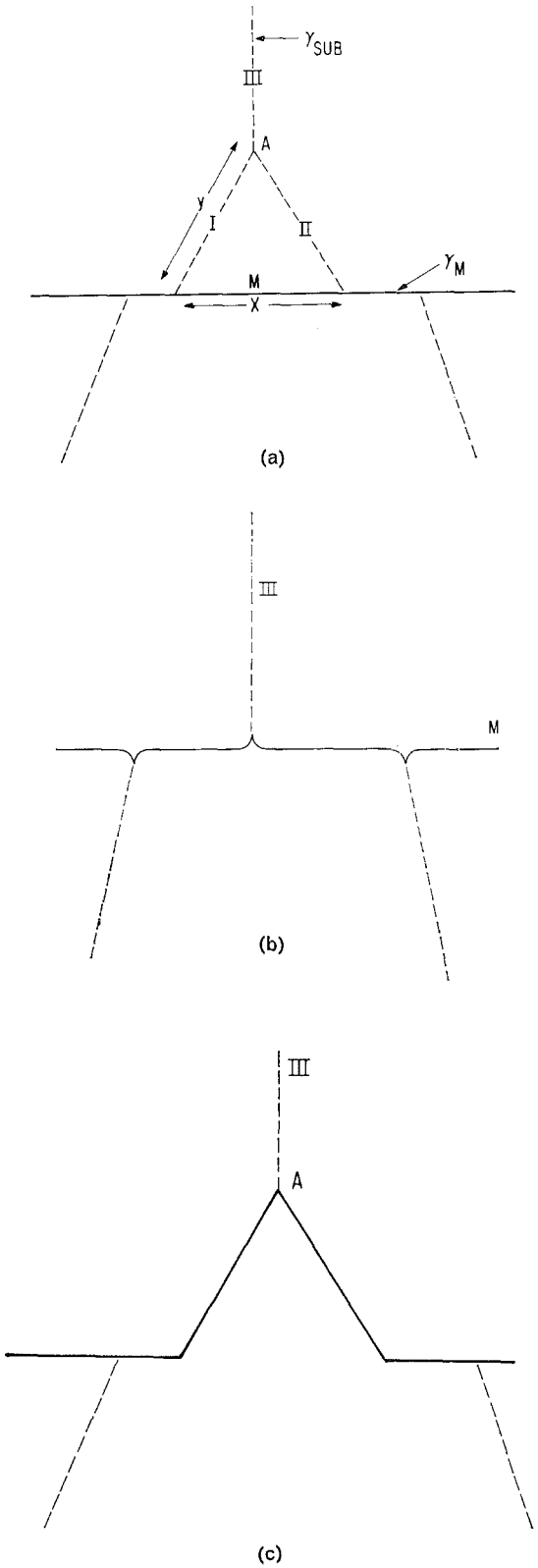

Figure 9 Interactions of substructure with a bicrystal boundary. (a) Unstable position of main boundary and sub-boundaries. (b) Equilibrium position of main boundary and sub-boundaries with similar mobilities. (c) Equilibrium position of mobile main boundary and immobile sub-boundaries. — — — —, sub-boundary; ——— main boundary.

severity of the ridging at high growth rates may be accounted for.

An alternative explanation of the moulding of the main boundary to the substructure morphology may be the following: it is well known that projections on the bottom of a graphite boat and on the underside of its cover can be used to trap a boundary [12]. In a similar fashion, sub-boundary grooving [20] at the solid-liquid interface may also tend to trap the main boundary and force it to conform to the substructure present in the crystal during crystal growth.

4.2. Aluminium

The origin and change of grain-boundary ridging with growth speed in aluminium can be explained in essentially the same manner as it was for zinc. Like zinc, substructure forms parallel to the solidification direction in aluminium crystals grown from the melt [13, 20] and the subgrain size decreases with increasing solidification rate [20]. Although there are some differences between zinc and aluminium in their substructure configurations [19, 20], the resulting ridging effects on their grain-boundary surfaces are taken to be identical. Similar ridging has also been observed on boundary surfaces of tin crystals grown from the melt [1]. Thus, the phenomenon of grain-boundary ridging appears to be associated with a wide range of crystal structures and angles of misorientation of the boundary and is probably typical of all metals which contain substructure originating in the solidification process.

The observed persistency of grain-boundary ridging in aluminium, even after prolonged annealing near its melting point, is the result of the fact that the substructure introduced during solidification is very stable. The lack of ridging on boundaries of recrystallised grains is a direct result of the fact that the recrystallised grains contain little, if any, substructure [22, 23] as compared to the as-cast grains.

4.3. Effects on Creep

For comparable grain-size and morphology, it

has often been observed that materials in the cast condition are generally more creep resistant than materials that have been wrought and annealed. For example, Rhines and his co-workers [24] found that as-cast aluminium bicrystals exhibited about one-third the rate of extension and grain-boundary sliding shown by strain-annealed bicrystals of a similar mis-orientation and purity. Since the results of the present investigation indicate that the principal difference between the as-cast and strain-annealed grain-boundaries is the presence of ridging in the former and its lack in the latter, it appears that grain-boundary ridging imparts a considerable degree of resistance to grain-boundary sliding and creep. This study thus suggests that the creep resistance of materials, in which grain-boundary sliding contributes to the creep process, may be improved by: (i) using materials in the as-cast condition; (ii) solidifying a material so as to have the direction of solidification perpendicular to the eventual direction of the applied stress [8] (i.e. shear stress across instead of parallel to the corrugations); (iii) using high solidification rates.

The amount of resistance to grain-boundary sliding that boundary ridging imparts has been estimated by Brunner and Grant [25] using slipline field analysis for a rigid plastic solid. τ, the shear stress necessary to cause grain-boundary sliding on a corrugated boundary (fig. 10a) in a rigid plastic solid with a yield stress k, is given in equation 1 as a function of α, the angle the corrugations make with an imaginary flat grain-boundary plane. In the derivation of equation 1, the assumption has been made [26] that the stress necessary to cause sliding along a perfectly flat boundary is zero.

$$\tau = k\left(\frac{\pi}{2} - 2\alpha + 1\right)\tan\alpha\,. \qquad (1)$$

Equation 1 is plotted in fig. 10b. Note that even with boundary corrugations, the shear stress necessary for grain-boundary sliding is still less than the shear stress required for general shear within the grains, provided that the ridging angle α is less than 45°. Thus, in the case of a ridging angle less than 45°, plastic flow would only occur in a zone around the grain-boundary the thickness of which is of the order of the height of the ridges. In order for grain-boundary ridging to impart its maximum resistance to creep, the ridging angle must exceed 45°. In such a case, general plastic deformation would occur within

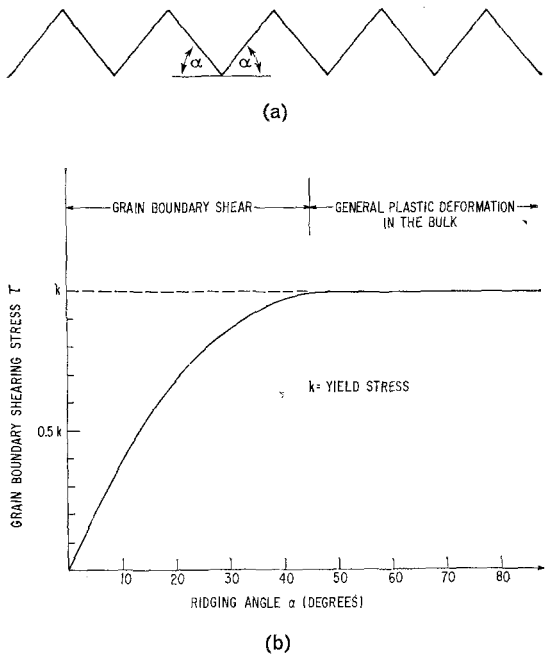

Figure 10 (a) Corrugated grain-boundary and its ridging angle α. (b) The shear stress necessary to cause grain-boundary sliding in a rigid plastic solid as a function of the boundary ridging angle α.

the grains at the same stress necessary for grain-boundary shear (fig. 10b). For a real material, the above description will probably provide an approximate picture of the initial stage of the creep process. Beyond this initial stage, such factors as work-hardening and the destruction of the boundary structure by plastic flow will invalidate many of the assumptions made above.

Although grain-boundary ridging in as-cast samples may impart a considerable amount of creep resistance to materials susceptible to grain-boundary sliding, ridging possibly may make a material more liable to creep rupture in the later stages of creep. Creep rupture most usually occurs by the nucleation and growth of cavities on grain-boundaries. McLean has stated that two sites in materials have been positively identified as places for cavity nucleation, namely, grain-boundary triple junctions and cusps in grain-boundaries produced by intersecting sub-boundaries [27]. Nevertheless, the effect of distributing stress over a large number of boundary ridges may be such that the stress concentration at individual ridges or triple junctions is kept below the critical stress needed to nucleate such cavities, thereby actually improving creep rupture properties.

Finally, grain-boundary ridging may cause a directional anisotropy in grain-boundary sliding rates. The grain-boundary sliding rates in the solidification direction (parallel to the ridging) would be larger than the grain-boundary sliding rate perpendicular to the solidification direction (across the ridging). Thus, Anthony and Walter [8] have suggested the grain-boundary ridging induced by solidification as an explanation of the anisotropic grain-boundary sliding rates observed by Horton and Beevers [2] in zinc bicrystal boundaries grown from the melt. An equally likely explanation of these anisotropic grain-boundary sliding rates could be the equilibrium faceting of some zinc bicrystal boundaries observed by Bishop *et al* [28, 29]. However, Horton and Beevers have recently presented evidence that grain-boundary ridging is not a factor in the anisotropic sliding rates observed in their zinc bicrystals [30].

5. Conclusions

Grain-boundaries of high purity aluminium and zinc bicrystals grown from the melt are not flat. The extent of deviation from flatness depends upon the rate of crystal growth and ranges from broad facets at low rates of growth to deep ridges or corrugations at high rates. The direction of ridging is parallel to the solidification direction. The facets and ridges are formed as a result of the interaction of the high-angle bicrystal boundary with the low-angle substructure boundaries.

The presence of the ridges should impart resistance to grain-boundary sliding in directions not parallel to the direction of ridging and, thus, may impart creep resistance to materials in which grain-boundary sliding contributes to the creep process.

Acknowledgement

The authors are grateful to D. Lee for his critical reading of the manuscript. The light micrographs were prepared by the members of the Metallographic Unit.

References

1. K. E. PUTTICK and R. KING, *J. Inst. Met.* **80** (1951) 537.
2. C. A. P. HORTON and C. J. BEEVERS, *Acta Met.* **16** (1968) 733.
3. K. E. PUTTICK and B. TUCK, *ibid* **13** (1965) 1043.
4. F. WEINBERG, *ibid* **2** (1954) 889.
5. F. WEINBERG, *Trans. AIME* **212** (1958) 808.
6. J. L. WALTER and H. E. CLINE, *ibid* **242** (1968) 1823.
7. K. E. PUTTICK and R. KING, *J. Inst. Met.* **8b** (1951) 1378.
8. T. R. ANTHONY and J. L. WALTER, *Scripta Met.* **3** (1969) 281.
9. B. FAZAN, O. D. HERBY, and E. J. DORN, *Trans. AIME* **200** (1954) 919.
10. D. MCLEAN, "Creep and Fracture of Metals at High Temperatures" (NPL Symposium, London, 1954) p. 73.
11. B. CHALMERS, *Proc. Roy. Soc.* **A175** (1940). 100
12. R. L. FLEISCHER and R. S. DAVIS, *Trans. AIME* **215** (1959) 665.
13. P. E. DOHERTY and B. CHALMERS, *ibid* **224** (1964) 1124.
14. I. S. SERVI and N. F. GRAVES, *ibid* **212** (1958) 315.
15. J. REZEK and B. CRAIG, *ibid* **221** (1961) 715.
16. K. F. HULME, *Acta Met.* **2** (1954) 810.
17. J. W. RUTTER, "Liquid Metals and Solidification" (ASM Cleveland, Ohio, 1957) p. 265.
18. I. K. ZASIMCHUK and D. E. OVSIENKO, "Growth of Crystals" (Plenum Publishing Corp, New York, 1968) p. 73.
19. J. REZEK and B. G. CRAIG, *Can. J. Phys.* **40** (1962) 674.
20. D. JAFFREY and G. A. CHADWICK, *Phil. Mag.* **18** (1968) 573.
21. J. W. RUTTER and K. T. AUST, *Acta Met.* **13** (1965) 181.
22. A. GUINIER and J. TENNEVIN, *Prog. Met. Phys.* **2** (1950) 177.
23. M. N. PARTHASARATHI and P. A. BECK, *Trans. AIME* **212** (1958) 821.
24. F. N. RHINES, W. E. BOND, and M. A. KISSEL, *Trans. ASM* **48** (1956) 919.
25. H. BRUNNER and N. J. GRANT, *Trans. AIME* **215** (1959) 48.
26. H. HENCKY, *Z. angew. Mat und Mech* **3** (1923) 241.
27. D. MCLEAN, *J. Inst. Met.* **93** (1964-65) 320.
28. G. H. BISHOP, W. H. HARTT, and G. A. BRUGGEHAM, submitted to *Acta Met.* (1969); *J. Metals* **20** (1968) 71a.
29. F. WEINBERG, *Trans AIME* **245** (1969) 2009.
30. C. A. P. HORTON and C. J. BEEVERS, *Scripta Met.* **3** (1969) 285.

Received 22 July and accepted 6 October 1969.